Supplementary material for:
Variability in high-throughput ion-channel screening data and consequences for cardiac safety assessment

Ryan C. Elkins, Mark R. Davies, Stephen J. Brough,
David J. Gavaghan, Yi Cui, Najah Abi-Gerges, Gary R. Mirams

April 25, 2013

Contents

1 S   Supplementary Material

2 S.1   High-throughput screening protocol details

3 In the following sections we provide full experimental protocol details for
4 the IonWorks Quattro screens performed at AZ (S.1.1) and GSK (S.1.2),
5 together with the GSK FLIPR screen (S.1.3). All recordings were made at
6 room temperature.

7 S.1.1   AstraZeneca IonWorks screens

8 These details in this section are as in Davies et al. (2012, Table 1), as the
9 screens were undertaken by the same team at AstraZeneca, using the same
10 procedure as that study.

11 Cell culture

12 Cells expressing hKv11.1 (hI$_{\text{ERG}}$):
13 Cells[1] were grown in Hams F-12 nutrient mixture and L-glutamine sup-
14 plemented with 10% FCS and 600μg/ml Hygromycin. Cells used in the
15 IonWorks were incubated at 37℃ for 24 h and then incubated at 28℃ for
16 48–72 h.

17 Cells expressing hNaV1.5 (hI$_{\text{Na}}$):
18 Cells[1] were grown in Hams F-12 nutrient mixture and glutamax supple-
19 mented with 10% FCS and 1,000μg/ml geneticin. Cells used in the Ion-
20 Works were incubated at 37℃ for 24 h and then incubated at 28℃ for 24
21 h.

22 Cells expressing hKv4.3/hKChIP2.2 (hI$_{\text{to}}$):
23 Cells[1] were grown in Hams F-12 nutrient mixture and glutamax supple-
24 mented with 10% FCS, 1,100μg/ml geneticin, and 600 μg/ml hygromycin.
25 Cells used in the IonWorks were incubated at 37℃ for 24 h, then at 28℃
26 for 48 h.

27 Cells expressing hKvLQT1/hminK (hI$_{\text{Ks}}$):
28 Cells purchased from Millipore were grown in Iscoves nutrient mixture and
29 Glutamine supplemented with 10% FCS, 400μg/ml geneticin, 100μg/ml

---

[1]Cells were described by Persson et al. (2005b) and Persson et al. (2005a). All cells
were grown to semiconfluence at 37℃ in a humidified environment (5% CO$_2$).

hygromycin, 2% HT supplement (50×), and 1% nonessential amino acids (100×). Cells used in the IonWorks were incubated at 37℃ for 48 h.

Cells expressing hCav1.2(hI$_{Ca}$):
Cells purchased from Chantest Corporation were grown in Hams F-12 nutrient mixture and L-glutamine supplemented with 10% FCS, blasticidin (10μg/ml), geneticin (G-418, 400μg/ml), hygromycin (250μg/ml), penicillin-streptomycin (100 units/ml; 100μg/ml), and zeocin (75μg/ml). Twenty-four hours before assay cells were induced with doxycycline to a final concentration of 1μg/ml and incubated for a further 68 h at 37℃. They were then incubated at 28℃ overnight.

Preparation of cells for IonWorks

Cells expressing hI$_{ERG}$ and hI$_{Na}$[2]:
After the monolayer of cells was detached with Versene solution (~3 ml, 1:5,000), cells were washed with PBS (Dulbecos phosphate containing Ca^{2+}/Mg^{2+}) and centrifuged at 50 g for 4 min. The supernatant was discarded and the remaining pellet of cells was resuspended in of PBS. For hI$_{ERG}$ (IonWorks) and hI$_{Na}$ (Quattro) measurements, cell concentrations of 0.25×10^6 cells/ml and 1×10^6 cells/ml were used, respectively.

Cells expressing hI$_{to}$[2] and hI$_{Ks}$:
The method used was the same as that prescribed above, except for the following changes: cells were washed with PBS (no Ca^{2+}/Mg^{2+}) and incubated with 0.05% Trypsin/EDTA solution. Both cell lines were adjusted to 1×10^6 cells/ml (both run in Quattro mode).

Cells expressing hI$_{CaL}$:
After the monolayer of cells was washed with PBS, cells were detached with accutase and centrifuged at 1,100 g for 2 min. The supernatant was discarded and the remaining pellet of cells was resuspended in HBPS containing 10 mM BaCl2 (HBPS + Ba) to a concentration of 1.5 million cells/ml.

Measurements of currents

Cells are incubated for 3 minutes in the presence of a compound before acquiring the ion current data post-compound addition.

---

[2]When performing the CHO-hI$_{Na}$/CHO-hI$_{to}$ duplex assay, the cell counts were determined and the cell concentration for both cell suspensions was adjusted to 1×10^6 cells/ml. The cells were mixed together to attain a 60:40 ratio hI$_{Na}$:hI$_{to}$. A single voltage pulse was applied to evoke the pre- and post-compound currents, and the degree of inhibition or stimulation was assessed by dividing the postscan current by the respective prescan current for each well.

hI_{ERG}:
A holding potential of -70mV was applied for 20 s, followed by a 160 ms step to -0mV (allowing an estimated leak current to be measured), and a 100 ms step back to -70mV. The voltage was then stepped to $+40$mV for 1 s and a steady-state current was observed. A 2 s step down to -30mV, inducing the tail current, was then followed by a 0.5 s step to -70mV.

hI_{Ks}:
The voltage protocol consisted of a 5 s period holding at -80mV, a 100 ms step to -100mV (to measure an estimated leak current), a 100 ms step back to -80mV, followed by a 4 s step to $+40$mV, a 300 ms step to -40mV, and finally a 200 ms step to -80mV.

hI_{Na} and hI_{to}[3]:
The voltage protocol consisted of a 15 s period holding at -90 mV, a 160ms step to -100mV (to measure an estimated leak current), a 100 ms step back to -90mV, followed by 10 pulses each for a duration of 50 ms applied at 3 Hz. The first eight 50 ms pulses were to -20mV and the ninth and tenth pulses to $+20$ mV. 300 ms after the tenth pulse there was another longer pulse to $+20$ mV (1 s) with a final 300 ms step to -90 mV.

hI_{CaL}:
A holding potential of -65 mV was applied for 10 s, before depolarizing to 0mV for 500 ms and a steady-state current observed.

Solutions

hI_{ERG}, hI_{Ks}, hI_{Na}, and hI_{to}:
The internal solution was composed of (in mM) 100 K-gluconate, 40 KCl, 3.2 $MgCl_2$, 3 EGTA , and 5 HEPES (pH 7.3 using 1 M KOH). The access solution was composed of (in mM) 140 KCl, 1 EGTA, 1 $MgCl_2$, and 20 HEPES (pH 7.3 using 1 M KOH), and 100 μg/ml of amphotericin B. PBS contains (in mM) 136.9 NaCl, 2.7 KCl, 8 Na_2HPO_4, 1.5 KH_2PO_4, 0.9 $CaCl_2 0.2H_2O$, and 0.5 $MgCl_2 0.6H_2O$.

hI_{CaL}:
Similarly to the other four currents, same internal solution was used. The access solution was composed of (in mM): KCl 140, EGTA 1, $MgCl_2$ 1 and HEPES 20 (pH 7.3 using 1 M KOH), 4 mM escin, 2 mM K_2ATP and 0.3 mM Na_2GTP. HBPS contains (in mM): 135 NaCl, 4 KCl, 10 HEPES, 10

[3]The degree of response for hI_{Na} current was assessed for both the first and eighth pulses, while the effect on hI_{to} was assessed for the eleventh pulse.

95 Glucose 1 $MgCl_2 0.6H_2O$, pH 7.4.

Positive controls

97 hI_{ERG}:

98 Cisapride was solubilized in DMSO at a concentration of 3mM and further
99 diluted in PBS to make a top test concentration of $10\mu M$.

100 hI_{Na} and hI_{to}:

101 Flecainide was solubilized in DMSO at a concentration of 95mM and further
102 diluted in PBS to make a top test concentration of $31.6\mu M$.

103 hI_{Ks}:

104 XE991 was solubilized in DMSO at a concentration of 9.5mM and further
105 diluted in PBS to make a top test concentration of $31.6\mu M$.

106 hI_{CaL}:

107 Verapamil was solubilized in DMSO at a concentration of 316mM and fur-
108 ther diluted in HPBS + Ba^{2+} to make a top test concentration of $100\mu M$.

Serial dilutions

110 hI_{ERG}, hI_{Ks}, hI_{Na}, hI_{to}, and hI_{CaL}:

111 Each test compound was solubilized and serially diluted 7 times by half $\log_{10}$
112 units in DMSO as stock solutions. Each of these concentrations was then
113 further diluted 100-fold in PBS (HBPS + Ba^{2+} for hI_{Ca}) in a 96-well plate.
114 Each compound was then diluted threefold in PBS (HBPS + Ba^{2+} for hI_{Ca})
115 in the PatchPlate to give the final test concentrations.

Data Analysis

117 IonWorks data were either IC50 or EC50 value from one or more runs (Table
118 3). For each run, a noncumulative 8-point concentration-effect curve was
119 produced and an IC50 or EC50 value was determined, with data for a given
120 concentration of compound being from between 1 and 8 wells. When two
121 or more runs were performed then the data were merged before fitting a
122 Hill curve from which a single IC50 or EC50 value was derived. Data were
123 normalized to vehicle (0.1% DMSO), and the differences between vehicle and
124 top concentration tested were assessed for statistical significance using the
125 Students t-test and showing greater than 25% change from control (being
126 the amount needed to observe a difference beyond the experimental noise).
127 Where an antagonistic effect was observed with a compound, the data were
128 then fitted to a simple pore block model using the Hill equation, allowing the
129 Hill coefficient to vary but assuming that the compound would eventually

cause complete block of the channel. Agonists were not considered in this study.

S.1.2   GlaxoSmithKline IonWorks screens

Cell preparation

Human NaV1.5:

Human embryonic kidney-293 (HEK293) cells were stably transfected with human NaV1.5 expression vector (pCIN5-hNaV1.5). Cells were cultured in DMEM with F12, supplemented with 10% FBS, 1x NEAA, plus $400\mu g/ml$ geneticin. Cells were grown and maintained at 37℃ in a humidified environment containing 5% CO_2. Media without geneticin was used for cell harvesting. Cells with less than 80% confluency were detached from the T75 culture flask for passage and harvesting using TrypLE or Versene. After media aspiration cells were washed with pre-warmed Ca^{2+}- and Mg^{2+}-free D-PBS. Then 3 ml pre-warmed TrypLE or Versene were added for 3–5 min, respectively, followed by addition of 10–12 ml pre-warmed Ca^{2+}- and Mg^{2+}-containing D-PBS. Finally cells were gently mixed 3–4 times. The suspension was centrifuged at 300 x G for 2 minutes, the pellet resuspended to a cell concentration of of 2–3 million cells/ml and that solution added to the IonWorks™ instrument.

hERG:

Chinese hamster ovary (CHO) cells stably expressing hERG were cultured in M1 DMEM Hams with F12, supplemented with 10% FBS and $400\mu g/ml$ geneticin. Cells were thawed in T175 flasks at 6–8 million cells per T175 flask, maintained at 37℃ in a humidified environment containing 5% CO_2 for 3–4 hours and transferred to a 30℃ incubator containing 5% CO_2 and incubate for another 72 hrs before assaying. On day of assay, cells which were over 80% confluence were used. Media were removed and cells were washed with warm PBS (without magnesium and calcium) two times. 5ml pre-warmed Versene was added for 6 min, followed by addition of 10ml of warm M1 media. The suspension was placed into a 15ml centrifuge tube and spun for 2 min at 1K rpm. The supernatant was removed and cells were re-suspend in 5ml of warm M1 media and incubated for 5 mins for the cells to recover. After 5 mins the cells the suspension was centrifuged at 1K rpm for 2 mins, the pellet re-suspended to a cell concentration of 4–5 million cells/ml and that solution was added to the IonWorks™.

KCNQ1:

Chinese hamster ovary (CHO) cells were stably transfected with KCNQ1 (also known as Kv1.7 or KvLQT1) — the pore forming unit of the cardiac potassium current inward rectifier, and KCNE1 (also known as minK) the auxiliary subunit in the cariac ion channel. Cells were cultured in IMDM ISCOVE media, supplemented with 10% FBS and $800\mu g$/ml geneticin, 1ml hygromycin, 5ml Pen/Strep and filtered. Cells were thawed in T175 flasks at 6–8 million cells per T175 flask, maintained at 37℃ in a humidified environment containing 5% CO_2 for 24 hours and transferred to a 30℃ incubator containing 5% CO_2 and incubated for another 48 hrs before assaying. On day of assay, confluency of cells should be $< 40\%$ for screening. Media were removed, and cells were washed with warm KCNQ1 external solution (without magnesium and calcium). 3 ml pre-warmed TrypLE was added for 2–3 mins, followed by addition of 10 ml of warm KCNQ1 external solution (without magnesium and calcium). The suspension was placed into a 15 ml centrifuge tube and spun for 2 mins at 1K rpm. The supernatant was removed and cells re-suspended in 5 ml of warm KCNQ1 external solution (with magnesium and calcium). The pellet was re-suspended to a cell concentration of 3.5–4.5 million cells/ml and that solution added to the IonWorks™.

Experimental Protocols

All currents were recorded before and after the addition of compound using a Molecular Devices IonWorks Quattro automated electrophysiology instrument in Population Patch-Clamp mode.

Human NaV1.5:

The intracellular solution contained the following: 100mM K-gluconate, 40mM KCl, 3.2mM $MgCl_2$, 5mM HEPES, 3mM EGTA, pH 7.3 with KOH. Amphotericin-B solution was prepared as 50mg/ml stock solution in dimethylsulfoxide (DMSO) and diluted to a final working concentration of 0.1 mg/ml in intracellular solution. The external solution was D-PBS and contained the following: 0.90mM $CaCl_2$, 2.67mM KCl, 1.47mM KH_2PO_4, 0.493mM $MgCl_2$, 137.9mM NaCl, 8.06mM Na_2HPO_4, pH 7.4. All wells with a pre- and post-drug addition resistance of $> 20M\Omega$ and which yielded a > 200pA transient inward NaV current were included in the analysis.

The voltage pulse protocol applied pre- and post- compound addition was as follows: From a holding potential of -80mV (30 seconds), a train of five 200 millisecond depolarising voltage pulses were applied at a frequency of

2 Hz. The peak of the inward currents during the first and fifth 0 mV depolarisation were exported for the pre- and post-drug conditions. The amount of compound block observed at the fifth pulse determines the accumulated block observed and is expressed a percentage of the pre-compound current observed at the first pulse to give a measure of the "global" (tonic and use-dependent) block achieved by the compound.

hERG:

The KCl intracellular solution contained the following: 140mM KCl, 1mM $MgCl_2$, 1mM $CaCl_2$, 20mM HEPES, pH 7.3 with KOH. Amphotericin-B solution was prepared as 50mg/ml stock solution in dimethylsulfoxide (DMSO) and diluted to a final working concentration of 0.1 mg/ml in intracellular solution. The external solution was D-PBS (-). The voltage pulse protocol applied pre- and post- compound addition was as follows: hERG currents were activated by 4 sec depolarising pulse to +40mV from a holding potential of −80mV. The cells were then repolarised to −50mV to generate large outward tail currents for 5 sec.

KCNQ1:

The KCNQ1 internal solution contained the following: 100mM Potassium Gluconate, 54mM Potassium Chloride, 3.2mM $MgCl_2$, 5mM HEPES, pH 7.3 with KOH. All solutions were filtered before use. Amphotericin-B solution was prepared as 50mg/ml stock solution in dimethylsulfoxide (DMSO) and diluted to a final working concentration of 0.1mg/ml in intracellular solution. The KCNQ1 external solution with Ca^{2+} and Mg^{2+} contained the following: 65mM Sodium Gluconate, 70mM Sodium Chloride, 5mM Potassium Chloride, 0.5mM $MgCl_2$, 1mM $CaCl_2$, 5mM HEPES, pH 7.4 with NaOH. The KCNQl external solution without Ca^{2+} and Mg^{2+} contained the following: 65mM Sodium Gluconate, 70mM Sodium Chloride, 5mM Potassium Chloride, 5mM HEPES, pH 7.4 with NaOH. The voltage pulse protocol applied pre- and post- compound addition was as follows: From a holding potential of −80mV (100ms), test opener potential 0 mV for 4s, step to −10mV for 2s, holding potential −80mV for 5s, test blocker potential +50mV for 4s, step to −10mV for 2s. The amount of compound block observed at the end of the +50mV pulse and is expressed a percentage of the pre-compound current observed at the beginning of the +50mV pulse to give a measure of the tonic block achieved by the compound.

Data Analysis

Ionworks recordings are population patch measurements in which the av-

erage of the current across many cells is determined. Hence the word observation is used for a single concentration response curve. There could be several observations on a certain day.

Human NaV1.5:

Comparisons between pre-drug peak transient inward currents at the first pulse and post-drug peak transient inward currents fifth pulse were used to determine the global inhibitory effect of the compound. Data were normalised to the high and low controls. Low controls were wells in which 100μM tetracaine was added for the NaV1.5 blocker assay. High controls were wells in which only 1% DMSO was added for the NaV1.5 blocker assay. The normalised data were analysed by using ActivityBase software. The amount of NaV1.5 current inhibition observed at the fifth depolarising pulse after compound addition was expressed as a percentage of the peak current observed at the first pulse before compound addition and used to generate a global block concentration dose response.

hERG:

Data were normalised to the high and low controls. Low controls were wells in which 50μM Quinindine was added for the hERG blocker assay. High controls were wells in which only 1% DMSO was added for the hERG assay. The normalised data were analysed by using ActivityBase software. The amount of tonic block is calculated from peak (maximum tail current value). This value is amplitude of the peak tail current minus the steady state average value obtained at -50mV holding potential before the first voltage step to $+40$mV.

KCNQ1:

Data were normalised to the high and low controls. Low controls were wells in which an internal characterised full block compound was added for the KCNQ1 blocker assay. DMSO concentration in compound wells and high controls wells were only 0.25% for the KCNQ1 assay. The normalised data were analysed by using ActivityBase software. The current elicited at the end of the 50mV pulse is normalised to that at the start of the pulse and normalised to control data.

For all channels:

Concentration response data were derived using a four parameter concentration effect curve fitting procedure. pIC50 values and Hill coefficients were determined from these inhibition curves.

9

S.1.3 GlaxoSmithKline CaV1.2 FLIPR screen

Cell preparation

Human embryonic kidney-293 (HEK293) cells were stably transfected with the $\beta2a$ and the $\alpha2\delta1$ subunits of CaV1.2 (L-type calcium channel). Cells were cultured in DMEM HAMS-F12 +10% FBS. Cells were grown and maintained at 37℃ in a humidified environment containing 5% CO_2. 24 hours prior to assay media was removed and replaced with DMEM-F12 media supplemented with 10% FBS and containing 2.5% hIK and 5% alpha1C BacMam virus transduction reagents to the cell suspension. Cells with less than 80% confluency were detached from the T75 culture flask for passage and harvesting using TrypLE or Versene. Cells were resuspended in DMEM-F12 media supplemented with 10% FBS and seeded at 15,000 cells per well in clear-bottom, black-walled 384 well plates.

Experimental Protocol

Human CaV1.2 fluorescence was measured before and after the addition of a depolarising addition of 400mM KCl using a Molecular Devices 384 well fluorescent imaging plate reader (FLIPR).

Cell media was replaced with tyrodes salt solution supplemented with 20mM HEPES, 11.9mM $NaHCO_3$, 2.5mM probenecid, 0.01% Pluronic acid, $2.5\mu M$ Fluo4-AM (a calcium sensitive fluophore) and $250\mu M$ Brilliant Black (quenching solution) at pH7.4 and the cells were incubated at 37℃ in a humidified environment containing 5% CO_2 for 60 minutes. Compounds were prepared as serial dilution concentration response curves in DMSO before being diluted in tyrodes medium immediately prior to assay. Cells were incubated for 15 minutes in the presence of tyrodes buffer containing compounds of interest. Cell plates containing compounds were placed inside the FLIPR and changes in fluorescence measured (λ_{ex}=488nm, λ_{EM}=54nm) (Sullivan et al., 1999) before and after the addition of the depolarising solution.

Data Analysis

The timecourse of fluorescence across each well of the plate was measured before and after stimulation, and the maximum, minimum and basal values were extracted for further analysis.

Blockade of the transient increase in fluorescence caused by the influx of calcium through the activated calcium channel was used to determine the global inhibitory effect of the compound. Data (maximum minus minimum

310 divided by basal fluorescence value) were normalised to the high and low
311 controls. Low controls were wells in which 1mM nimodipine was added for
312 the CaV1.2 blocker assay. High controls were wells in which only 1% DMSO
313 was added for the CaV1.2 blocker assay. The normalised data were analysed
314 by using ActivityBase (IDBS) software. Concentration response data were
315 derived using a four parameter concentration-effect fitting procedure. pIC50
316 values were determined from these inhibition curves.

S.2   Choice of distributions

318 In order to decide the best distribution to describe the pIC_{50} datasets we
319 generated probability plots for a large range of distributions. Two common
320 distributions, that both showed a reasonable fit to the data, are the normal
321 distribution and the logistic distribution. In Figure S1 we show probability
322 plots for the large Cisapride hERG dataset and these two distributions. The
323 figure shows that pIC_{50} values follow a logistic distribution rather than a
324 normal distribution.

325 These findings appear to hold reasonably for all of the other assays and
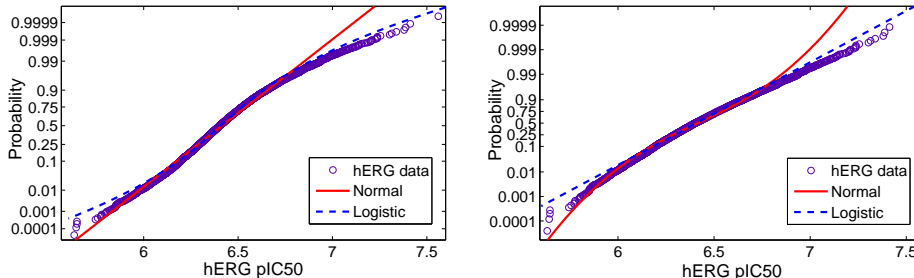326 control compounds that were considered, see Figures S2 and S3.

Figure S1: Probability plots for the hERG Cisapride IonWorks Quattro
dataset. Left: a normal distribution probability plot, the data
deviates from the straight line that a perfect normal distribu-
tion would follow. Right: a logistic distribution probability plot,
the data is closer to a straight line on this plot (although nearer
a normal distribution at lower pIC_{50} values), overall a logistic
distribution is a much better fit for these data.

327 To estimate the parameters of the distributions we used maximum likelihood
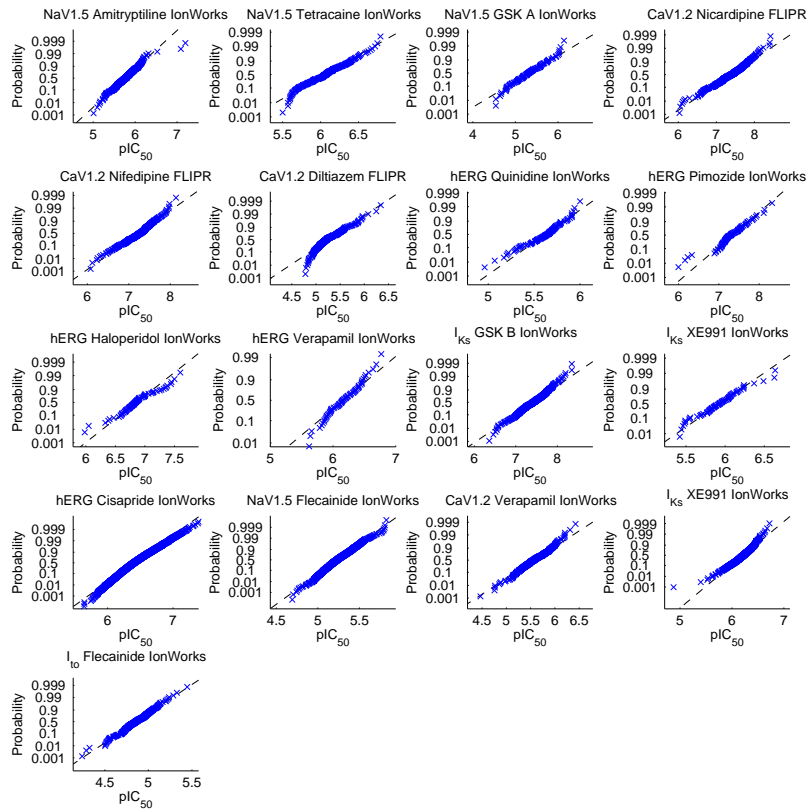328 estimates, provided by the MatLab™statistics toolbox 'mle' function (see

11

Figure S2: pIC$_{50}$ logistic distribution probability plots for all control datasets. Data points lying along the straight dashed line would indicate a perfect logistic distribution.
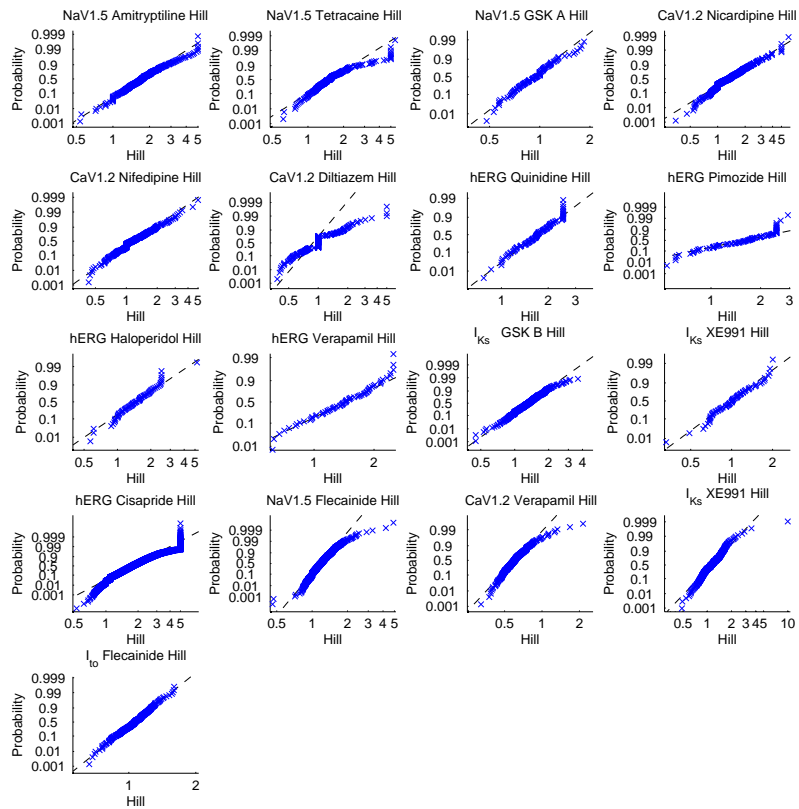
Figure S3: Hill log-logistic distribution probability plots for all control datasets. Data points lying along the straight dashed line would indicate a perfect log-logistic distribution.

13

Note that MatLab provides two log-logistic parameters that are equal to μ and σ from a corresponding logistic distribution, describing

$$ln(X) \sim \text{Logistic}(\mu, \sigma), \tag{1}$$

and to transform to the standard log-logistic parameters describing

$$X \sim \text{LogLogistic}(\alpha, \beta), \tag{2}$$

the conversion $\alpha = e^\mu$ and $\beta = 1/\sigma$ must be used. To perform the Bayesian inference described in equations (5) & (6) of the main text we need to evaluate the probability of a given observation for a certain distribution. For this we use the probability density function (PDF) for each distribution. These are given, in the standard notation, by

$$f(x; \mu, \sigma) = \frac{e^{-(x-\mu)/\sigma}}{\sigma(1 + e^{-(x-\mu)/\sigma})^2}, \tag{3}$$

for the logistic distribution; and

$$f(x; \alpha, \beta) = \frac{(\beta/\alpha)\,(x/\alpha)^{\beta-1}}{\left[1 + (x/\alpha)^\beta\right]^2}, \tag{4}$$

for the log-logistic distribution.

Figure S4 demonstrates how a consistent scaling parameter β does not prevent the spread of the log-logistic probability distribution (equation (4)) increasing for increasing median values α. This explains why the apparent increase in the spread of high Hill coefficients shown in Figure 6(a) of the main text, does not necessarily imply a larger scaling parameter (seen in Table 1). This phenomenon is not associated with the logistic distribution.

The spread parameters that were assumed to underlie the experimental observations used in the action potential simulations of Section 3.2 are shown in Table S1.
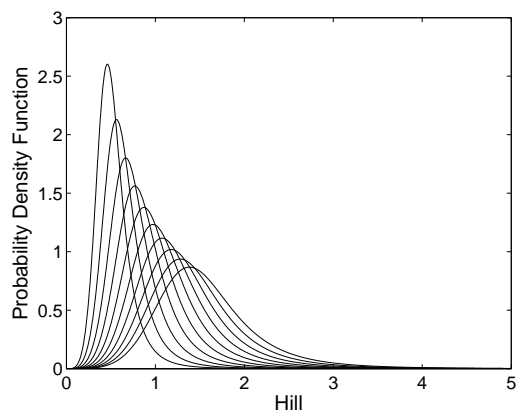
14

Figure S4: Probability density functions for the Hill coefficient (log-logistic) distribution. Despite the spread about the centre of the distribution increasing, the distribution scaling parameter is the same for each curve: equation (4) is plotted here for a varying median value $0.5 \leq \alpha \leq 1.5$ with a constant scaling parameter $\beta = 5$. These values are typical of the ones found in our assay results (see Table 1 of the main text).

Table S1: Spread parameters that were assumed to underlie the observed experimental data.

Ion channel	HTS platform	pIC$_{50}$ spread σ	Comments	Hill spread $1/\beta$	Comments
NaV1.5	IonWorks	0.076	From AZ control	0.084	From AZ control
CaV1.2	IonWorks	0.159	From AZ control	0.121	From AZ control
hERG	IonWorks	0.103	From AZ control	0.178	From AZ control
I$_{Ks}$	IonWorks	0.140	Averaged from all	0.166	Averaged from all
I$_{to}$	IonWorks	0.086	From AZ control	0.086	From AZ control

S.3 Bayesian inference calculation details

In order to simplify this section we discuss how estimates of the 'true' pIC_{50} value (μ) might be obtained, exactly the same procedure can be followed for estimates of the 'true' Hill coefficient (α) by substituting α for μ in the following discussion.

In order to implement the Bayesian inference scheme, we perform a discretization of the possible underlying continuum of possibilities for μ. In practice the necessary calculations are cheap for logistic and log-logistic distributions, and so in what follows we choose 10^6 distinct possible (i and j) values, giving a high resolution on the resulting probability distributions. Let us say this gives a spacing of $\Delta\mu$ between each discrete value of μ that is considered. In a slight abuse of notation — since the probability of observing any particular value μ_i is vanishingly small — we use $P(\mu_i \mid x)$ to represent the probability of the underlying μ being in the range $\mu_i - \frac{\Delta\mu}{2} < \mu < \mu_i + \frac{\Delta\mu}{2}$, given the observed data x.

We use Bayes' Theorem to calculate the likelihood of distributions with a particular median pIC_{50} value (μ_i) giving rise to the observed pIC_{50} (x). In equation format:

$$P(\mu_i \mid x) = \frac{P(x \mid \mu_i)P(\mu_i)}{\sum_{\forall j} P(x \mid \mu_j)P(\mu_j)}. \tag{5}$$

Evaluating equation (5) for all of our possible choices of μ_i gives us a distribution for the possible μ values. This distribution describes the probability of the corresponding pIC_{50}-centred distribution giving rise to the observed experimental data. Note here that there is a 'prior', $P(\mu_i)$, in equation (5). For pIC_{50} values we choose a uniform prior on $[-12, 12]$. The prior is the probability of observing a given μ_i value before considering the data x. Our prior implies that any pIC_{50} between -12 and $+12$ is equally likely, and that no value outside these can be taken. We perform the same analysis for α in the case of Hill coefficients, with our prior being uniform on $[0.1, 10]$. The sum on the denominator is a discretised version of an integral, that is used for the numerical computation.

The pIC_{50} values considered during drug development and safety testing may be an average of a small number of individual HTS assays. In this case equation (5) can be adapted to calculate the probability of observing 'n' independent recordings (represented by $\mathbf{x} = [x_1, x_2, \ldots, x_n]$, and indexed by

16

k) as follows:

$$P(\mu_i \mid \mathbf{x}) = \frac{\prod_{\forall k} P(x_k \mid \mu_i) P(\mu_i)}{\sum_{\forall j} \prod_{\forall k} P(x_k \mid \mu_j) P(\mu_j)}. \tag{6}$$

If repeat experiments yield similar values (as the results in section 3.1 suggest), their effect is to reduce the effective spread of the $P(\mu_i \mid \mathbf{x})$ distribution. We therefore tend to obtain a narrower distribution for the 'true' pIC$_{50}$ values when multiple experiments are performed, as shown in Figure 3 of the main text.

We convert the resulting probability density function for μ to an inverse cumulative distribution function numerically, and therefore gain a method for converting random numbers between 0 and 1 into samples of μ that may have given rise to the observed data. This is the method used in Section 2.4.2 of the main text.

There was little, if any, correlation between IC$_{50}$ and Hill for any of the assays, as can be seen in Figure S5. We therefore obtained samples from the respective distributions independently.
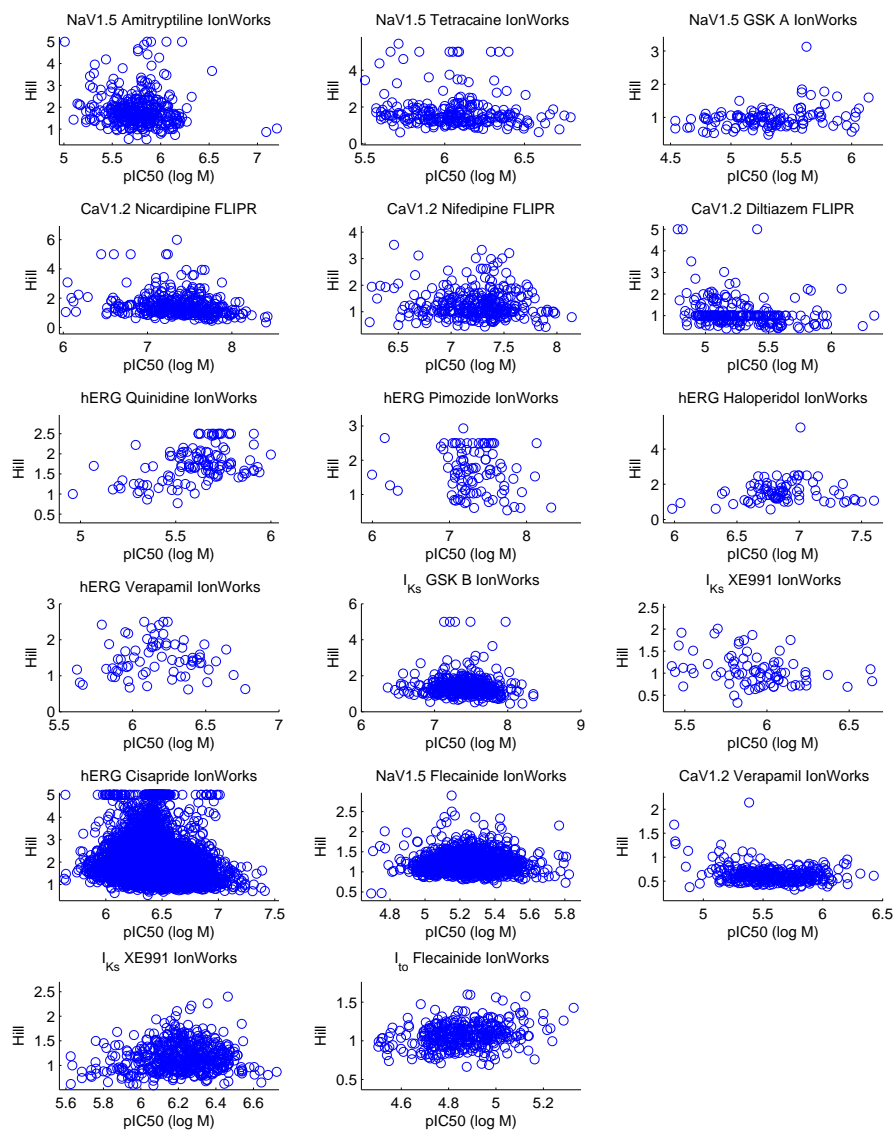
17

Figure S5: Scatter plots of the individual pIC_{50} values and Hill coefficients for each control assay. The lack of correlation suggests that the two can be treated as independent for sampling purposes.

S.4 Expanded results: histograms of pIC_{50} and Hill coefficients

S.4.1 IonWorks Quattro: hERG

Full histograms and fits for each compound are shown in Figures S6 and S7. The histogram for Cisapride is shown in Figure 2 of the main text.
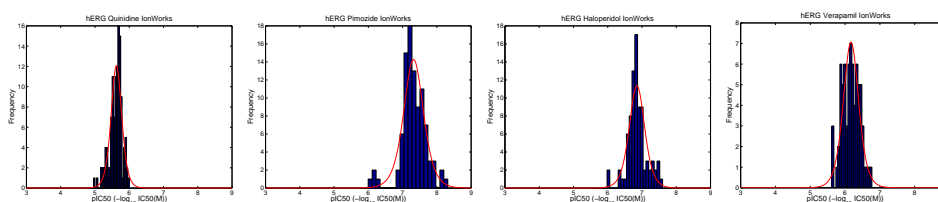

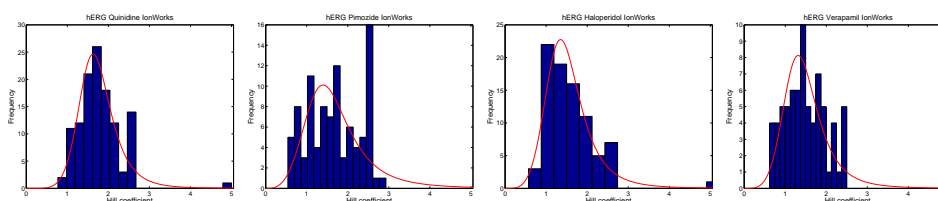Figure S6: pIC_{50} histograms for all IonWorks hERG controls.

Figure S7: Hill coefficient histograms for all IonWorks hERG controls.

S.4.2 IonWorks Quattro: I_{CaL}

Full histograms and fits for each compound are shown in Figure S8.

S.4.3 FLIPR: I_{CaL}

Full histograms and fits for each compound are shown in Figures S9 and S10.

S.4.4 IonWorks Quattro: I_{Na}

Full histograms and fits for each compound are shown in Figures S11 and S12.
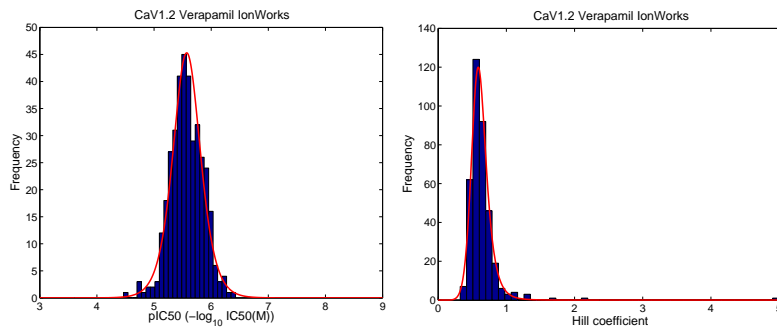
Figure S8: pIC_{50} and Hill histograms for IonWorks CaV1.2 control.
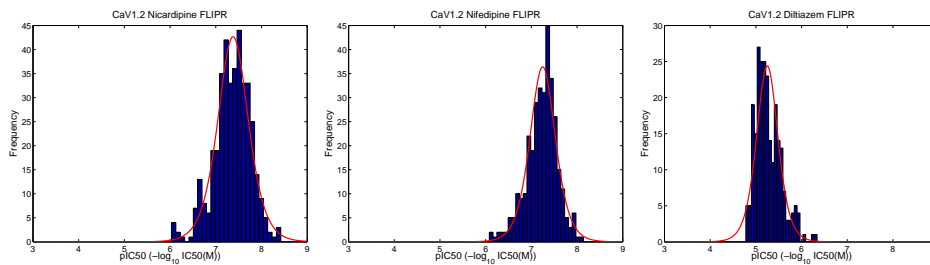

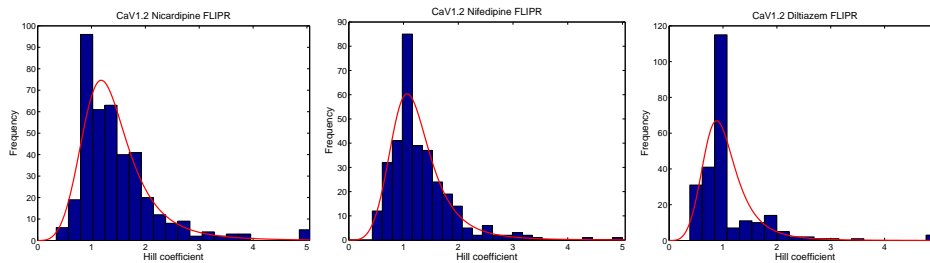Figure S9: pIC_{50} histograms for all FLIPR CaV1.2 controls.

Figure S10: Hill coefficient histograms for all FLIPR CaV1.2 controls.

S.4.5 IonWorks Quattro: I_{Ks}

Full histograms and fits for each compound are shown in Figures S13 and S14.

Figure S11: pIC$_{50}$ histograms for all IonWorks NaV1.5 controls.

Figure S12: Hill coefficient histograms for all IonWorks NaV1.5 controls.
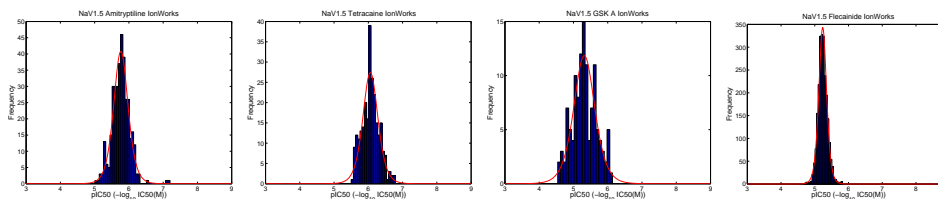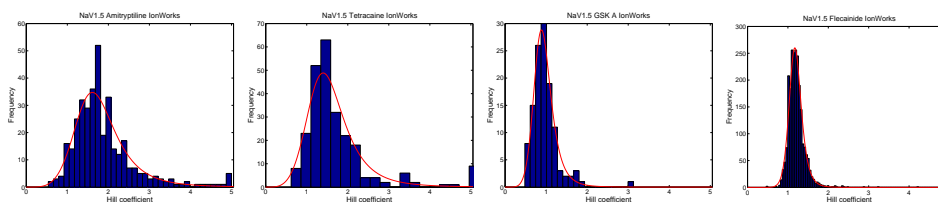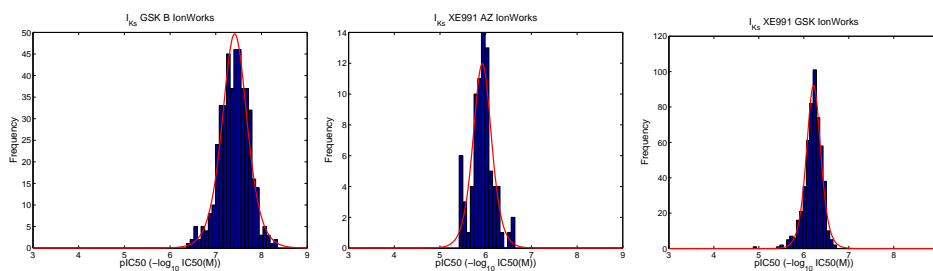

Figure S13: pIC$_{50}$ histograms for all IonWorks KCNQ1/minK controls.
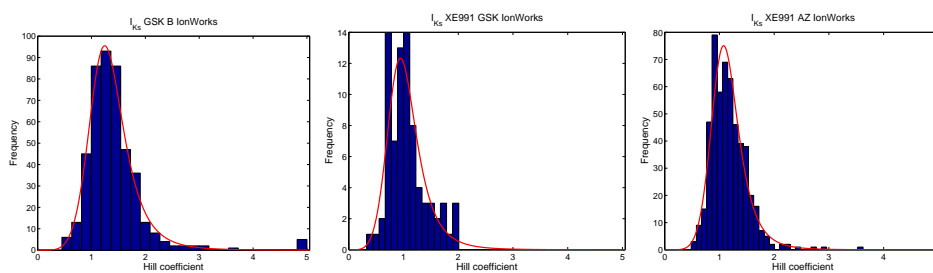
Figure S14: Hill coefficient histograms for all IonWorks KCNQ1/minK controls.

S.4.6 IonWorks Quattro: I$_{to}$

Full histograms and fits for each compound are shown in Figure S15.
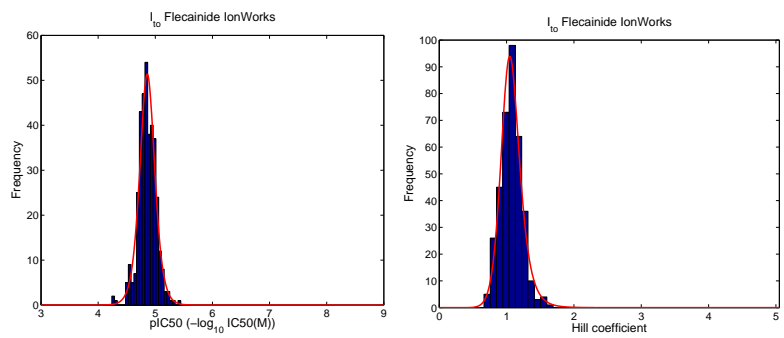
Figure S15: pIC_{50} and Hill histograms for IonWorks I_{to} control.

S.5 Expanded results: simulations

Space limitations in the main paper mean that tables analagous to those for Alfuzosin in the main text's Table 3 & 4 are presented here for the compounds: Dofetilide (Tables S2 & S3); Lacosamide (Tables S4 & S5); Nilotinib (Tables S6 & S7); and Tolterodine (Tables S8 & S9). The results presented in these tables are discussed in section 3.2 of the main text.

Table S2: Uncertainty in concentration-effect curves for action potential duration under the action of Dofetilide, when considering ion-channel assay variability in pIC_{50} values (not in Hill coefficients), for various numbers of repeats. Each plot displays action potential duration, APD_{90}, as a function of concentration. Black lines represent simulation results for each set of sampled concentration-effect inputs, the red line denotes the result when using the numbers reported by the assay directly, with 95% credible intervals imposed.

N	hERG variability	hERG/NaV1.5/CaV1.2 variability	hERG/NaV1.5/CaV1.2/ I_{Ks}/I_{to} variability
1			
2			
4			
8			
	Concentration (μM)	Concentration (μM)	Concentration (μM)

24

Table S3: Uncertainty in concentration-effect curves for action potential duration under the action of Dofetilide, when considering ion-channel assay variability in pIC_{50} values and Hill coefficients, for various numbers of repeats. Each plot displays action potential duration, APD_{90}, as a function of concentration. Black lines represent simulation results for each set of sampled concentration-effect inputs, the red line denotes the result when using the numbers reported by the assay directly, with 95% credible intervals imposed.

N	hERG variability	hERG/NaV1.5/CaV1.2 variability	hERG/NaV1.5/CaV1.2/ I_{Ks}/I_{to} variability
1	APD_{90} (ms)		
2	APD_{90} (ms)		
4	APD_{90} (ms)		
8	APD_{90} (ms) Concentration (μM)	Concentration (μM)	Concentration (μM)

Table S4: Uncertainty in concentration-effect curves for action potential duration under the action of Lacosamide, when considering ion-channel assay variability in pIC_{50} values (not in Hill coefficients), for various numbers of repeats. Each plot displays action potential duration, APD_{90}, as a function of concentration. Black lines represent simulation results for each set of sampled concentration-effect inputs, the red line denotes the result when using the numbers reported by the assay directly, with 95% credible intervals imposed.
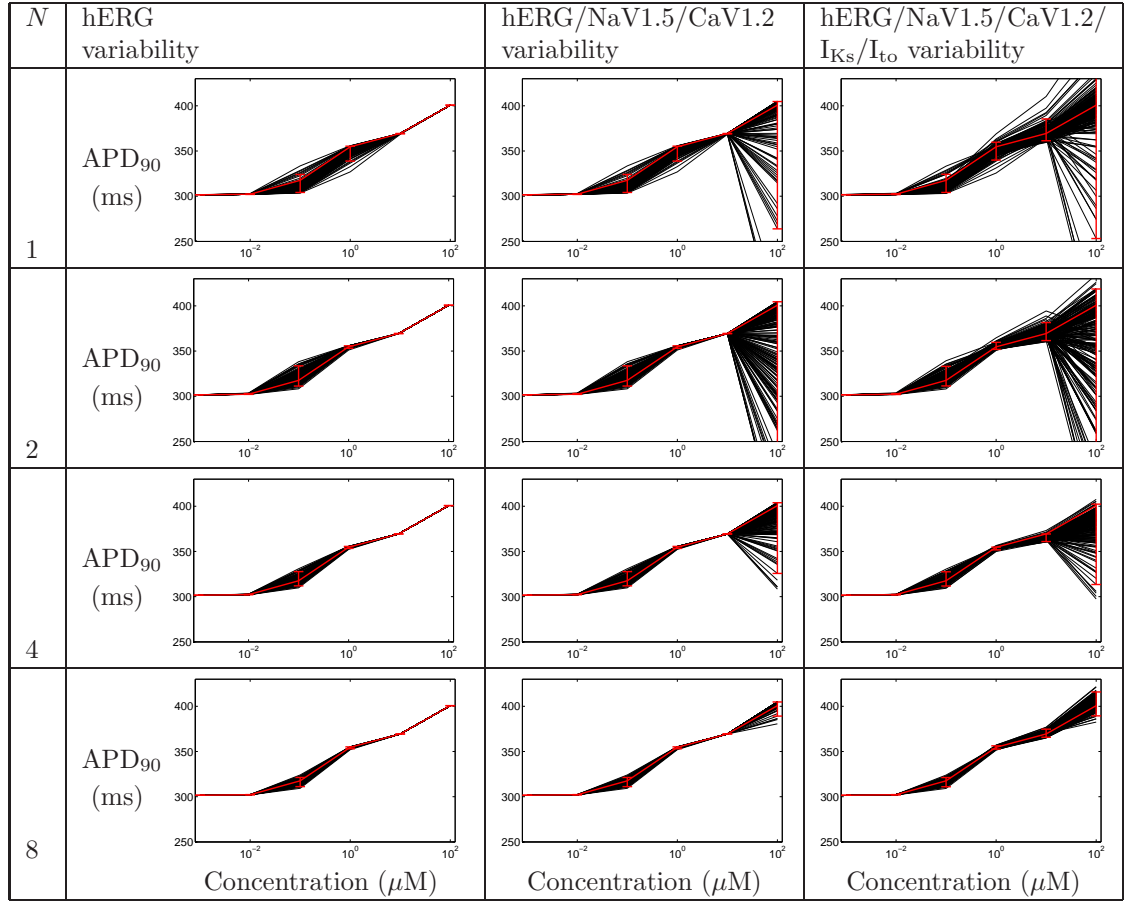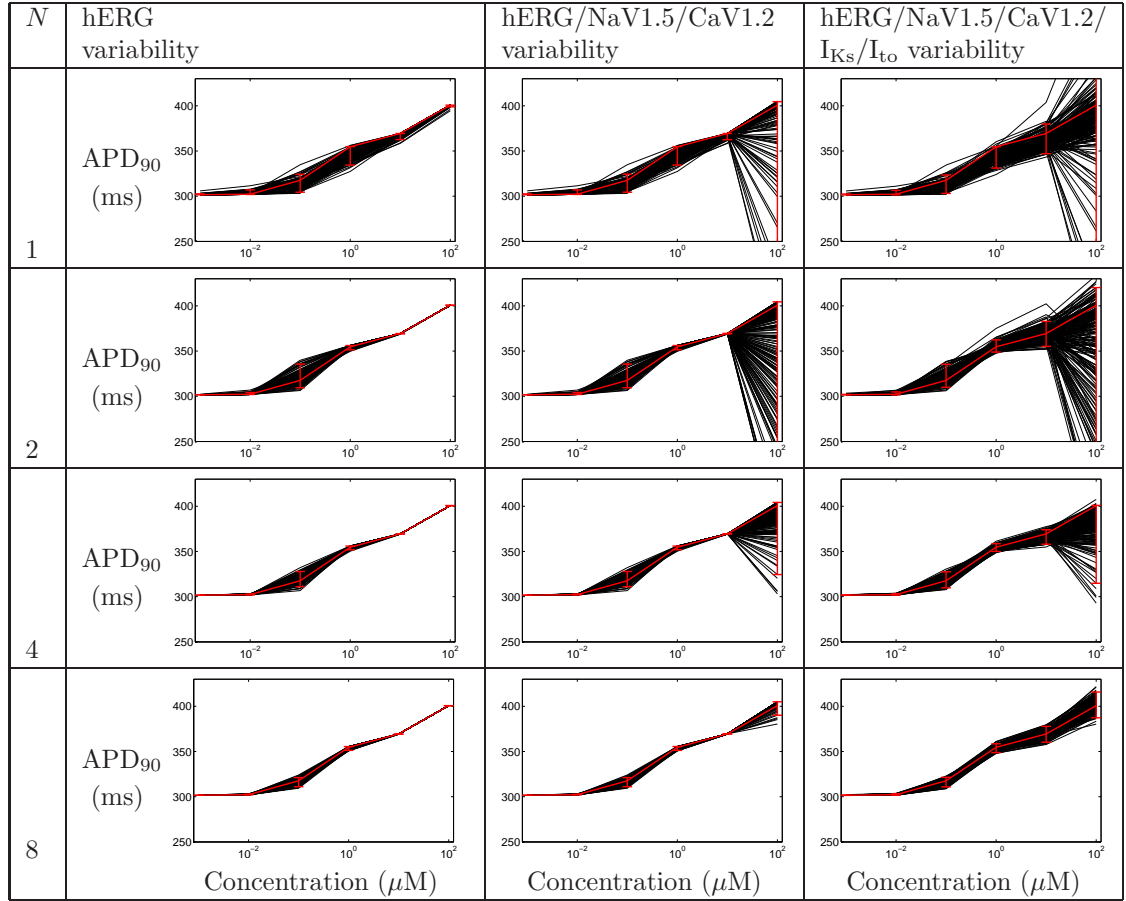
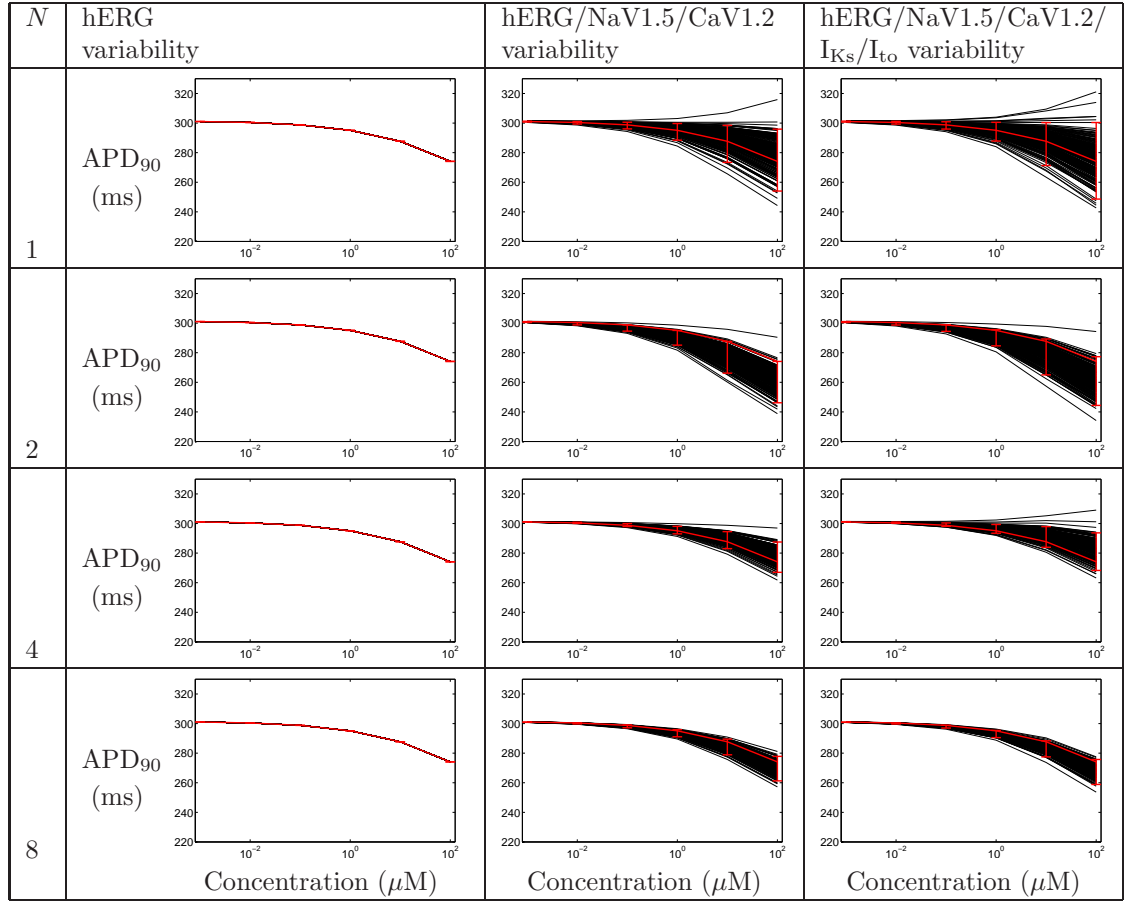| N	hERG variability	hERG/NaV1.5/CaV1.2 variability	hERG/NaV1.5/CaV1.2/ I_{Ks}/I_{to} variability
1	APD_{90} (ms)		
2	APD_{90} (ms)		
4	APD_{90} (ms)		
8	APD_{90} (ms)		
	Concentration (μM)	Concentration (μM)	Concentration (μM)

Table S5: Uncertainty in concentration-effect curves for action potential duration under the action of Lacosamide, when considering ion-channel assay variability in pIC_{50} values and Hill coefficients, for various numbers of repeats. Each plot displays action potential duration, APD_{90}, as a function of concentration. Black lines represent simulation results for each set of sampled concentration-effect inputs, the red line denotes the result when using the numbers reported by the assay directly, with 95% credible intervals imposed.

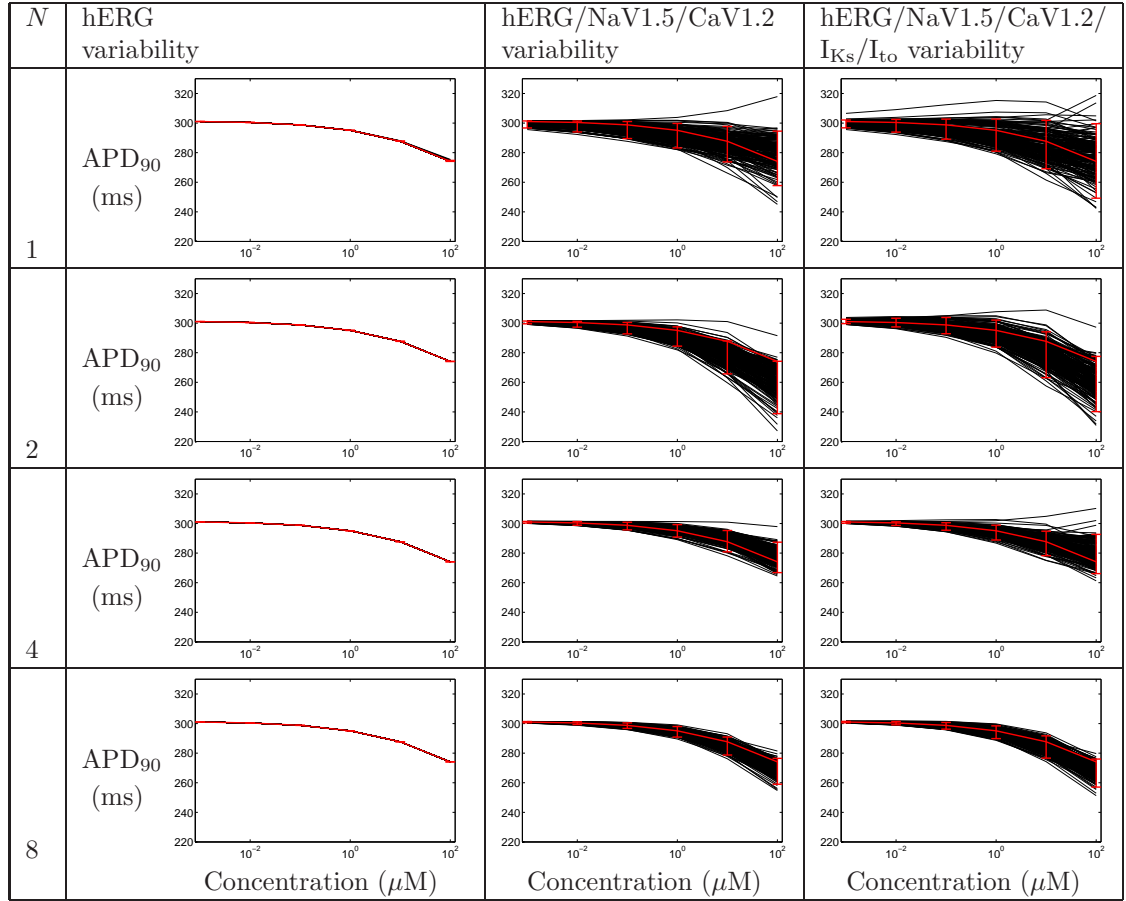| N	hERG variability	hERG/NaV1.5/CaV1.2 variability	hERG/NaV1.5/CaV1.2/ I_{Ks}/I_{to} variability
1	APD_{90} (ms)		
2	APD_{90} (ms)		
4	APD_{90} (ms)		
8	APD_{90} (ms)	Concentration (μM)	Concentration (μM)	Concentration (μM)

Table S6: Uncertainty in concentration-effect curves for action potential duration under the action of Nilotinib, when considering ion-channel assay variability in pIC_{50} values (not in Hill coefficients), for various numbers of repeats. Each plot displays action potential duration, APD_{90}, as a function of concentration. Black lines represent simulation results for each set of sampled concentration-effect inputs, the red line denotes the result when using the numbers reported by the assay directly, with 95% credible intervals imposed.

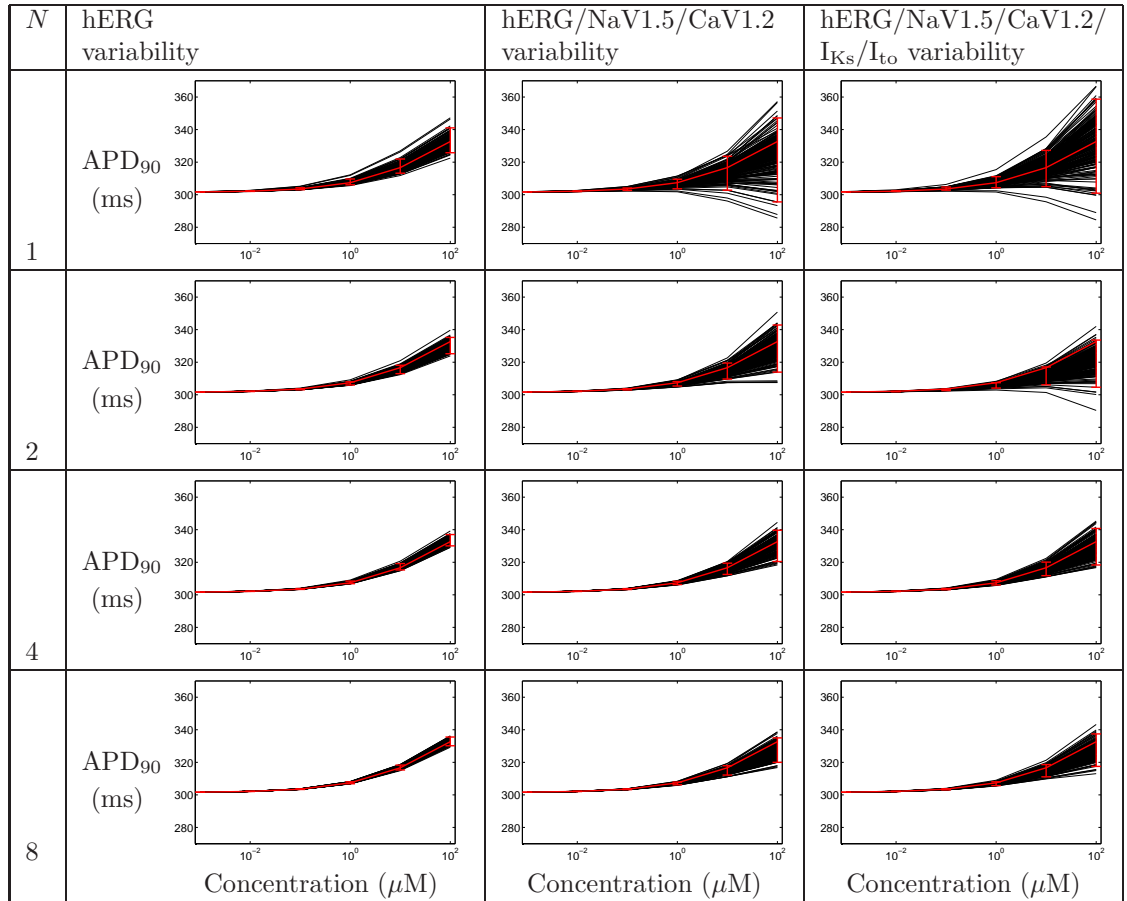| N	hERG variability	hERG/NaV1.5/CaV1.2 variability	hERG/NaV1.5/CaV1.2/ I_{Ks}/I_{to} variability
1			
2			
4			
8			

Table S7: Uncertainty in concentration-effect curves for action potential duration under the action of Nilotinib, when considering ion-channel assay variability in pIC_{50} values and Hill coefficients, for various numbers of repeats. Each plot displays action potential duration, APD_{90}, as a function of concentration. Black lines represent simulation results for each set of sampled concentration-effect inputs, the red line denotes the result when using the numbers reported by the assay directly, with 95% credible intervals imposed.
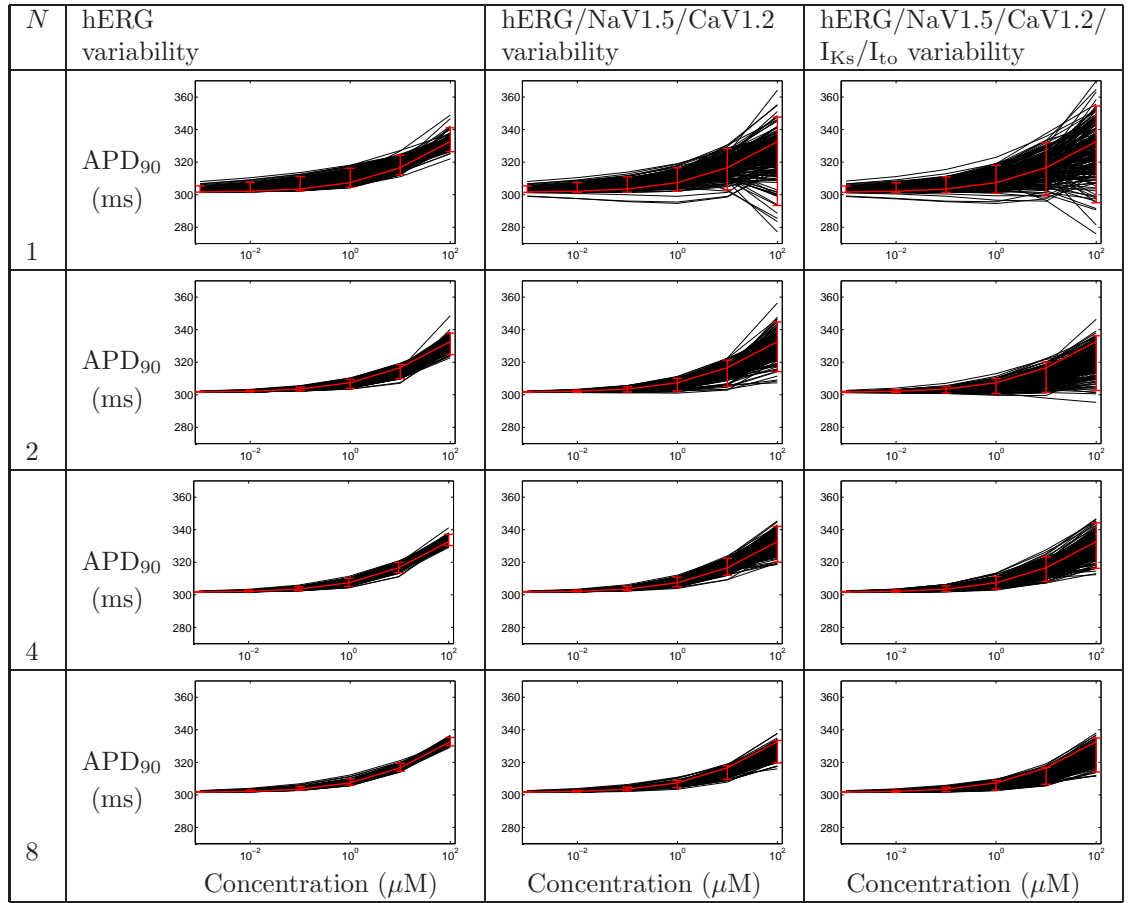
Table S8: Uncertainty in concentration-effect curves for action potential duration under the action of Tolterodine, when considering ion-channel assay variability in pIC_{50} values (not in Hill coefficients), for various numbers of repeats. Each plot displays action potential duration, APD_{90}, as a function of concentration. Black lines represent simulation results for each set of sampled concentration-effect inputs, the red line denotes the result when using the numbers reported by the assay directly, with 95% credible intervals imposed.

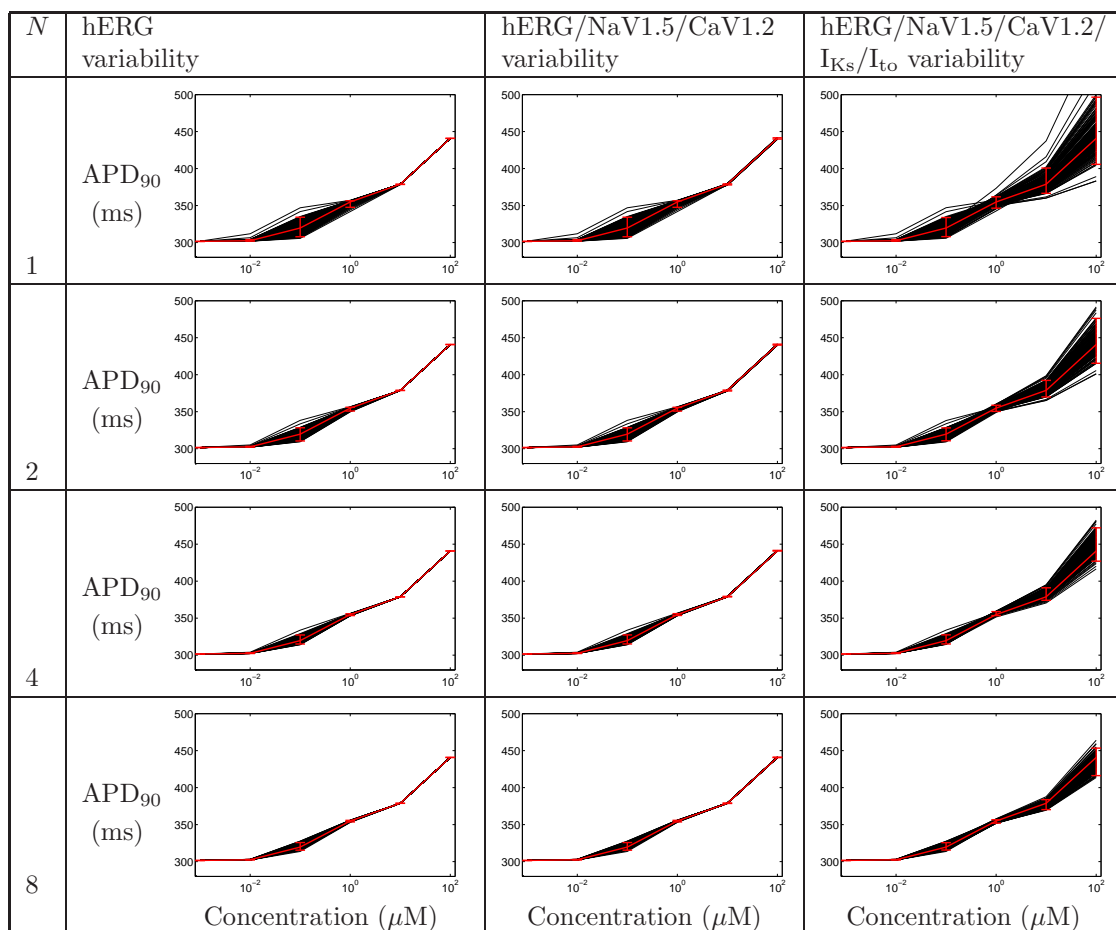| N	hERG variability	hERG/NaV1.5/CaV1.2 variability	hERG/NaV1.5/CaV1.2/ I_{Ks}/I_{to} variability
1	APD_{90} (ms)		
2	APD_{90} (ms)		
4	APD_{90} (ms)		
8	APD_{90} (ms) Concentration (μM)	Concentration (μM)	Concentration (μM)

Table S9: Uncertainty in concentration-effect curves for action potential duration under the action of Tolterodine, when considering ion-channel assay variability in pIC_{50} values and Hill coefficients, for various numbers of repeats. Each plot displays action potential duration, APD_{90}, as a function of concentration. Black lines represent simulation results for each set of sampled concentration-effect inputs, the red line denotes the result when using the numbers reported by the assay directly, with 95% credible intervals imposed.

N	hERG variability	hERG/NaV1.5/CaV1.2 variability	hERG/NaV1.5/CaV1.2/I_{Ks}/I_{to} variability
1			
2			
4			
8			
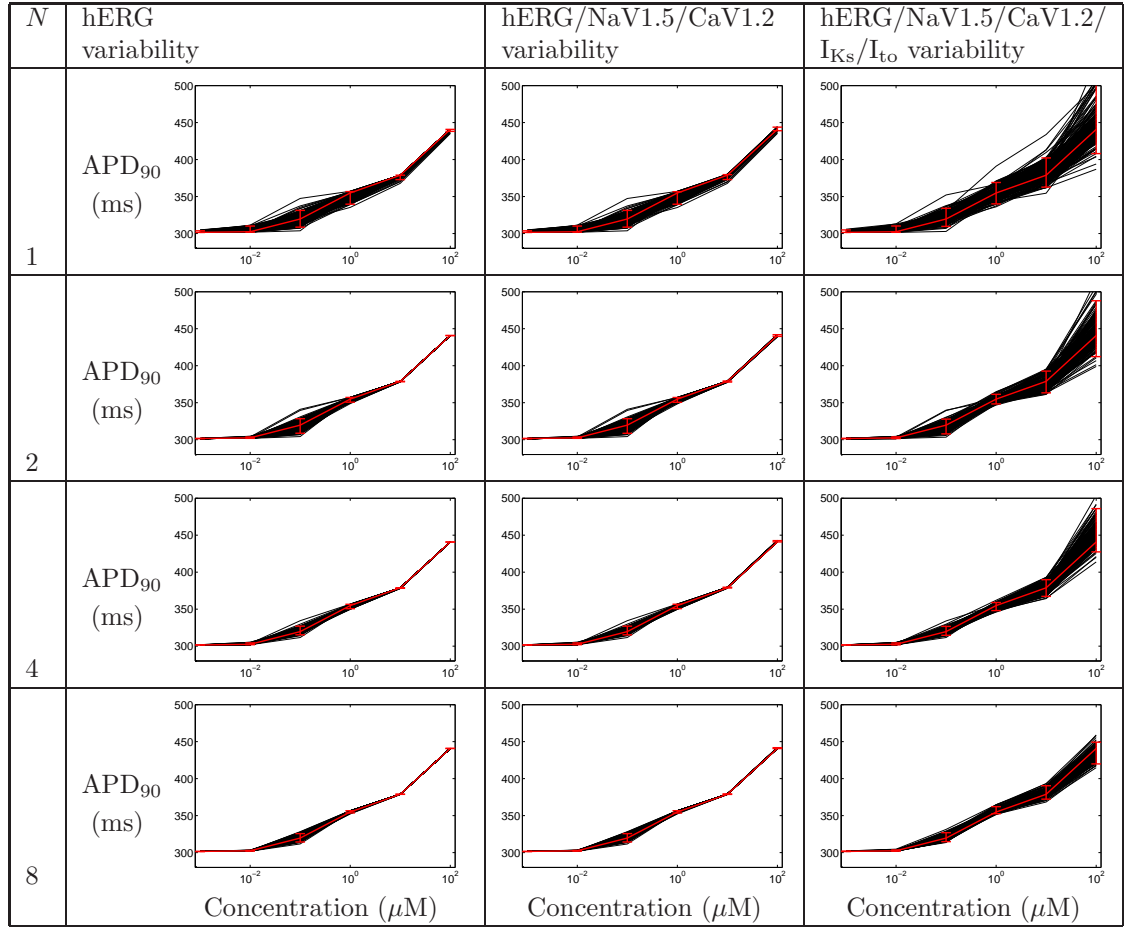
References

Davies, M., Mistry, H., Hussein, L., Pollard, C., Valentin, J.-P., Swinton, J., Abi-Gerges, N., 2012. An in silico canine cardiac midmyocardial action potential duration model as a tool for early drug safety assessment. American Journal of Physiology - Heart and Circulatory Physiology 302 (7), H1466–H1480.

Persson, F., Carlsson, L., Duker, G., 2005a. Blocking characteristics of hKv1.5 and hKv4.3/hKChIP2.2 after administration of the novel antiarrhythmic compound AZD7009. Journal of cardiovascular pharmacology 46 (1), 7–17.

Persson, F., Carlsson, L., Duker, G., Jacobson, I., 2005b. Blocking Characteristics of hERG, hNav1. 5, and hKvLQT1/hminK after Administration of the Novel Anti-Arrhythmic Compound AZD7009. Journal of cardiovascular electrophysiology 16 (3), 329–341.

Sullivan, E., Tucker, E., Dale, I., 1999. Measurement of [ca2+] using the fluorometric imaging plate reader (flipr). In: Lambert, D. (Ed.), Calcium Signaling Protocols. Vol. 114 of Methods in Molecular Biology. Humana Press, pp. 125–133.